Earth and Planetary Science Letters 591 (2022) 117603

Contents lists available at ScienceDirect

Earth and Planetary Science Letters

www.elsevier.com/locate/epsl

Oxygen isotope insights into the Archean ocean and atmosphere

Haley C. Olson *, Nadja Drabon, David T. Johnston

Harvard University Department of Earth and Planetary Sciences, 20 Oxford St, Cambridge, 02138, MA, United States of America

ARTICLE INFO

Article history:
Received 2 February 2022
Received in revised form 28 April 2022
Accepted 9 May 2022
Available online 26 May 2022
Editor: B. Wing

Keywords:
Archean
sulfur
$\delta^{18}O$
$\Delta'^{17}O$

ABSTRACT

Accurately reconstructing the temperature of the ocean through time carries implications for Earth's climate and early habitability. Attempts to build these reconstructions using oxygen isotope records have led to three end-member interpretations. Namely, that the observed enrichment over time in ^{18}O relative to ^{16}O in ancient chemical sediments reflects a change in sea-surface temperatures (SST), a change in the ^{18}O composition of the contemporaneous water, or that the primary signal has been subsequently overprinted. These questions become most salient in the Archean, where estimates of the isotopic composition of the ocean span ~20‰, with a correspondingly wide range in estimated SSTs. Here, we introduce barite ($BaSO_4$) as a robust new proxy for the oxygen isotope composition of the Archean ocean. We compile new and existing triple oxygen isotope and sulfur isotope data from the Fig Tree Group barite deposits in the Barberton Greenstone Belt, South Africa, with the goal of identifying the primary sources of sulfate to the Archean ocean. Using a simple Monte Carlo approach, we then constrain the possible isotopic composition of contemporaneous seawater. Our results suggest that microbial sulfur cycling played a limited role in setting the isotopic composition of Archean seawater sulfate. Additionally, it is likely that a significant flux of sulfate to the marine reservoir was atmospherically derived and carried a significant positive triple oxygen isotope signal. Importantly, our results support an Archean ocean with a somewhat enriched oxygen isotope composition (~0-5‰), with the exact composition dependent on the relative contribution from each sulfate production pathway. This result points either to the decreased significance of low-temperature weathering and/or to elevated SSTs in the early Archean.

1. Introduction

Estimates for the temperature of the Archean ocean cover an ~80°C range (Kasting et al., 2006; Knauth and Epstein, 1976; Johnson and Wing, 2020; Krissansen-Totton et al., 2018), based on a variety of geochemical measurements and modeling approaches. One of the primary tools used to constrain this range is the temperature-dependent isotopic equilibrium that exists between water and many oxygen-bearing mineral species (Urey, 1947). The chemical sediments included in the debate center on the oxygen isotope composition of Archean chert (microcrystalline SiO_2; e.g., Knauth and Epstein, 1976), hydrothermally altered ocean crust (Johnson and Wing, 2020), and phosphate minerals (Blake et al., 2010), complemented by geophysical models that vary the nature of seawater-crust interactions (Kasting et al., 2006). Although each offer insight, these approaches are not without controversy.

Central to each of these approaches is the isotopic composition of Archean seawater. Importantly, applying an isotopic equilibrium leaves at least two unknowns: formation temperature, often the goal of these applications, and the $\delta^{18}O$ of seawater itself. For the latter, estimates range widely, from values as depleted as -14‰ (Jaffrés et al., 2007) to as enriched as +3.3‰ (Johnson and Wing, 2020). The $\delta^{18}O$ composition of seawater is largely set by the relative importance of high- versus low-temperature interactions with Earth's crust (Muehlenbachs, 1998; Kasting et al., 2006). The oxygen isotope composition of oceanic crust, which is considered an infinitely large reservoir, can be approximated as unaltered basaltic glasses, which have an average $\delta^{18}O$ of 5.8±0.3‰ (Muehlenbachs, 1998). High-temperature interactions between seawater and such material are thought to effectively buffer seawater to 0±2‰ (Muehlenbachs, 1998). Conversely, low-temperature water-rock interactions (i.e., off-axis seawater infiltration into oceanic crust) largely act to isotopically deplete seawater and have been used as a mechanism to explain the ^{18}O-depletion in Archean chemical sediments (Kasting et al., 2006). Accordingly, constraining the isotopic composition of Archean seawater would not only constrain the temperature of the system, but also the nature of seawater-crust interactions over Earth history.

* Corresponding author.
E-mail address: haleyolson@g.harvard.edu (H.C. Olson).

https://doi.org/10.1016/j.epsl.2022.117603
0012-821X/

These approaches to temperature reconstructions are complicated by the possibility that the chemical sediments that precipitated early in Earth history have since been isotopically overprinted by diagenentic exchange processes. In fact, triple oxygen isotope data (noted $\Delta'^{17}O$) suggest that the often-cited chert record has experienced secondary hydrothermal alteration by meteoric waters, leaving previous temperature estimates derived from this record inaccurate (e.g., Liljestrand et al., 2020; Sukanya Sengupta and Peter, 2020, for an alternative view, see Lowe et al., 2020). The utility of the triple oxygen isotope system in predicting the true $\delta^{18}O$ (and $\delta^{17}O$) of contemporaneous seawater lies in the specific predictions for temperature-dependent isotopic equilibrium within any given mineral-water system. That is, most low-temperature processes that occur on Earth's surface (abiotic or biotic) are mass-dependent, meaning they impart a predictable fractionation of $^{17}O/^{16}O$ that is ~0.5 times the fractionation of $^{18}O/^{16}O$ (e.g., Young et al., 2002; Cao and Liu, 2011). It is possible, then, to use the triple oxygen isotope composition of a mineral to disentangle the sources of oxygen to that mineral, be it primary or secondary (Liljestrand et al., 2020; Waldeck et al., 2019; Bindeman et al., 2019; Sharp et al., 2018). This tool, in conjunction with a mineral system that is particularly robust to secondary alteration, has the potential to independently constrain the oxygen isotope composition of seawater and the associated environmental conditions. Here, we propose that the triple oxygen isotope composition of Archean barite may offer such constraints.

Sulfate-bearing minerals are a powerful tool used in the reconstruction of Proterozoic and Phanerozoic environments (Claypool et al., 1980). Most recently, the triple oxygen isotope signature of barite ($BaSO_4$), as well as gypsum ($CaSO_4$-$2H_2O$) and anhydrite ($CaSO_4$), has been used to constrain changes in atmospheric chemistry and gross primary production through time (Paleoproterozoic to the modern; e.g. Crockford et al., 2018; Bao et al., 2008; Hodgskiss et al., 2019). Though a fraction of the oxygen atoms in these sulfate deposits is thought to be sourced from contemporaneous O_2, enabling the studies noted above, the majority of the oxygen reflects an equilibrium with ambient H_2O (Waldeck et al., 2019). Once formed, at low-temperatures and circumneutral pH, the sulfate anion does not exchange oxygen isotopes with ambient water (Lloyd, 1968). Further, the mineral barite is quite insoluble ($pK_{sp_{barite}}$=~10 at 25°C), making it less likely than other chemical sediments (e.g. $pK_{sp_{gypsum}}$=~4.5 at 25°C) to be subjected to secondary dissolution and reprecipitation and any isotopic resetting associated with these processes (Holser et al., 1979; Lloyd, 1968). As such, targeting barite may largely side-step concerns that plague other Archean chemical sediments. Here, we investigate the fidelity of Archean barite as a primary record of Earth surface environments using the Paleoarchean Fig Tree Group in the Barberton Greenstone Belt, South Africa. Decades of work has examined the Archean sulfur cycle using multiple sulfur isotopes (e.g., Farquhar et al., 2000; Muller et al., 2016; Bao et al., 2007), so here we develop an oxygen isotope-specific model of the Archean sulfur cycle that tracks the incorporation of oxygen into sulfate as a means to extract estimates of the oxygen isotope composition of Archean seawater.

2. Geological setting and sample locations

The Barberton Greenstone Belt (BGB; 3.6 to 3.2 Ga; Lowe and Byerly, 1999) contains some of the oldest, most well-preserved sedimentary material exposed on Earth's surface. The BGB, which comprises the Onverwacht, Fig Tree, and Moodies Groups, has been separated into four fault-bounded domains (Lowe and Byerly, 1999). This study focuses on barite deposits found within the sedimentary rocks of the Fig Tree Group in the so-called East Central Domain, specifically in the basal and middle Mapepe Formation in Barite Valley (see Fig. S1). The Mapepe Formation in Barite Valley strikes SW-NE, dips steeply, and is marked by a fault dividing the stratigraphic sequence into western and eastern structural belts. These structural belts likely have different source terranes and depositional environments (Drabon et al., 2019; Lowe, 2013). The samples in this study come from three primary locations (Areas 1-3 described in Lowe et al., 2019; Fig. S1): one from Eastern Barite Valley (EBV) and two from Western Barite Valley (WBV).

The Mapepe Formation in the EBV has been divided into five members, where members 1-4 broadly reflect a shallowing-upward cycle that starts with deep-water mudstones and transitions to intertidal environments over hundreds of meters, capped by a return to deeper-water mudstones in member 5 (Drabon et al., 2019). Member 4, which hosts the largest of the barite deposits in the EBV, is largely characterized by tuff, tuffaceous sedimentary rocks, barite, and jaspilite (Drabon et al., 2019). The depositional setting at the time of barite deposition has been described as an "orthochemical bank" (Lowe and Nocita, 1999): a paleo-high created by the outwash of a fan delta, the top of which provided the intertidal environments conducive to the precipitation of the observed chemical sediments (Drabon et al., 2019; Drabon and Lowe, 2021). Though the sedimentology of the WBV is not directly correlative to the EBV and is less well-studied, the sediments that host the barite deposits suggest a shallow-marine to terrestrial setting (Lowe et al., 2019). The shallow depositional environments would allow for the concentration of sulfate sourced from either the marine reservoir or the atmosphere, which will be discussed in greater detail below.

Despite the host sediments suggesting somewhat different source terranes and depositional environments on either side of Barite Valley, these barite deposits likely formed via broadly similar mechanisms. They show a similar vent-plug anatomy and are host to multiple barite facies: cauliform or mounded barite (Lowe et al., 2019; Heinrichs and Reimer, 1977), bladed barite, and barite sands (which show local cross-lamination; Lowe et al., 2019). A dated spherule layer (S2) associated with a meteorite impact constrains the Barite Valley deposits to ≤3.260 Ga (Byerly et al., 1996). In WBV, chert dikes have been interpreted to be the result of soft-sediment flow into large seafloor fractures caused by a meteorite impact (Lowe et al., 2019; Lowe, 2013; Drabon et al., 2019). In EBV, the S2 impact may have caused the reworking of a barite sand bed at the base of the formation but has not been linked to the formation of the local chert dikes or other structures (Lowe et al., 2019; Lowe, 2013; Drabon et al., 2019).

Since barite is virtually insoluble, these deposits require the admixture of a Ba^{2+}-rich fluid with a SO_4^{2-}-bearing fluid from separate sources. These particular barite deposits are thus likely the result of relatively cool hydrothermal fluids rising along fault zones which terminated at the sea floor and which contained barium leached from underlying siliclastic and volcanoclastic material (Lowe et al., 2019). These fluids would have been injected into overlying waters, where sulfate was titrated out of the water column (Lowe et al., 2019). There is no evidence that the barite is a secondary replacement mineral, nor are there significant coexisting sulfide minerals within the deposits, indicating that subsequent dissolution/reprecipitation (perhaps via microbial cycling) did not occur (Lowe et al., 2019). The barite deposits found in the Mapepe Formation thus provide an ideal isotopic reservoir with which to constrain the isotopic composition of Archean ocean water.

3. Isotope nomenclature

We use standard isotope notation when reporting our results where the ratio of the minor oxygen isotope is reported relative to ^{16}O:

$$^{1X}R = \frac{^{1X}O}{^{16}O}, \quad (1)$$

which is extended to a delta notation given:

$$\delta^{17,18}O = 10^3\left(\frac{^{1X}R_{\text{sample}}}{^{16}R_{\text{VSMOW/SLAP}}} - 1\right). \quad (2)$$

Here, we normalize to a VSMOW/SLAP scale via a three-point calibration (air, NBS 28 and UWG2). This notation applies for sulfur isotope data as well:

$$\delta^{34}S = 10^3\left(\frac{^{34}R_{\text{sample}}}{^{32}R_{\text{VCDT}}} - 1\right), \quad (3)$$

here normalized to VCDT.

For simplicity, the triple oxygen isotope composition of a mineral is reported as the deviation in the ^{17}R composition from that predicted by ^{18}R. Each mass-dependent process generates a different isotope effect in ^{18}O and ^{17}O, which is expressed as θ and where:

$$^{17}R = \left(^{18}R\right)^{\theta}. \quad (4)$$

The associated triple oxygen isotope composition is expressed as:

$$\Delta'^{17}O_{\text{sample}} = 10^3(\ln(^{17}R) - \theta_{\text{RF}} * \ln(^{18}R)), \quad (5)$$

where θ_{RF} = 0.5305 and represents a high-temperature theoretical limit for equilibrium isotope exchange (Cowie and Johnston, 2016; Bao et al., 2016).

4. Methods

Fist-sized barite samples were recovered from unweathered surface outcrops (see sample locations in the SI) and were then processed using ion chromatography to ensure purity prior to isotopic analysis. Barite samples were first powdered by hand with a mortar and pestle and dissolved in a 0.05 M diethylenetriamenepentaacetic acid (DTPA) and 1 M NaOH solution on a shaker table for 72 hours. Different dissolution times (24 hours versus 72 hours) yielded no significant difference in the isotopic composition of the resulting material (see SI). After 72 hours, the DTPA solution (now containing chelated sulfate) was passed through ion chromatography columns packed with AG1-X8 anion exchange resin at a rate of ~1 mL/min and eluted with 0.4 N HCl. The resin was preconditioned with 3x20 mL of 3 M HCl and 3x20 mL of Milli-Q. To ensure quantitative precipitation, 5 mL of 1 M $BaCl_2$ was added to the resulting, post-column solution to precipitate $BaSO_4$, which was then rinsed three times in Milli-Q and left to dry overnight in an oven at 70°C. In-house standards run in parallel showed no triple oxygen isotope fractionation associated with sample processing.

Oxygen isotope measurements were made in the Johnston Lab at Harvard University. For δ^{18}O, approximately 0.25 mg of $BaSO_4$ along with approximately 0.50 mg of a graphite and $AgCl_2$ additive (2:1 mixture by weight) was weighed out for measurement in triplicate via a Thermo Finnigan TC/EA connected to a Delta V run in continuous flow mode. Data were drift- and scale-corrected and yielded an internal analytical precision (based on the weighted mean of standard materials) of 0.5‰ (1σ). Triple oxygen isotope measurements were obtained using laser fluorination coupled to a gas purification line (where analyte O_2 was thermally and chemically purified) and introduced to a Thermo MAT 253 Plus in dual inlet mode (following Cowie and Johnston, 2016). The O_2 yield from this method is not quantitative, so we tie our results to the δ^{18}O results from the TC/EA. All of the data published here have been corrected to a least-squares regression through the triple oxygen isotope composition of air and the IAEA silicate standards UWG-2 and NBS-28 (Wostbrock et al., 2020). The triple oxygen isotope data carry a weighted error of 0.02‰ (1σ) and are reported on a VSMOW/SLAP scale.

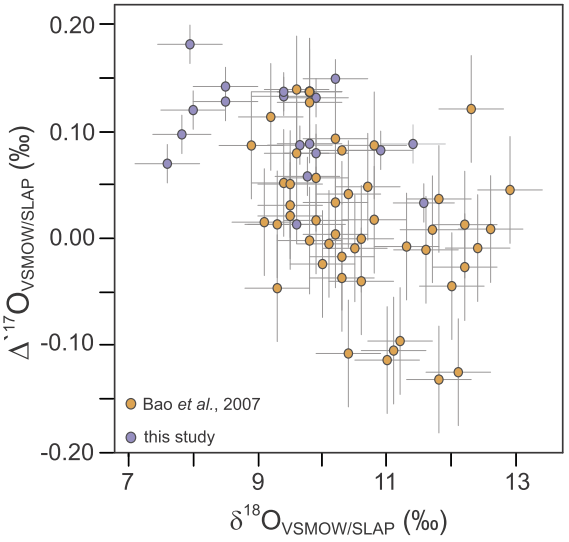

Fig. 1. A scatterplot showing the triple oxygen isotope data considered in this study, including barite measured for this study (purple) and barite measured previously (orange; Bao et al., 2007). Error bars represent the 1σ analytical uncertainty associated with each set of measurements. (For interpretation of the colors in the figure(s), the reader is referred to the web version of this article.)

Sulfur isotope measurements were made in the Gill Lab at Virginia Tech. For δ^{34}S, approximately 0.350 g of $BaSO_4$ along with ~5x the sample mass of V_2O_5 was weighed for measurement via an Elemental Analyzer coupled to a Isoprime 100 mass spectrometer operating in continuous flow mode. International standards IAEA-SO5, IAEA-SO6, and NBS 127 were run in parallel and yielded a weighted analytical error of 0.07‰ (1σ).

5. Results

The oxygen isotope composition of the Fig Tree Group barite covers a broad compositional range. The δ^{18}O composition ranges from 7.6‰ to 11.6‰, with mean δ^{18}O=9±1.2‰, while the Δ'^{17}O composition ranges from 0.03‰ to 0.18‰ with mean Δ'^{17}O=0.10± 0.04‰ (n=18; Fig. 1). The triple oxygen isotope data yield no correlation with facies (cauliform, bladed, or barite sand) nor with distance from the mouths of the vents (up to ~20 m away laterally). It is important to note that the vent morphology can be subvertical and, as we do not know the three-dimensional extent of these deposits, there are likely vents that remain unsampled. Though collected from multiple distinct vents, the data from each vent are statistically indistinguishable from one another. Statistically, these data may derive from a normally distributed population (Shapiro-Wilk test; p-value threshold=0.05; p-values=0.3 and 0.9 for δ^{18}O and Δ'^{17}O, respectively).

Sulfur isotope data from the Fig Tree Group barite range from 3.4‰ to 5.4‰ with a mean δ^{34}S=4.1±0.6‰. Similarly to the oxygen isotope data presented above, the sulfur isotope composition of the barite show no correlation with facies or location and is within the same range as previously published Fig Tree Group values (e.g., 3.7 to 6.2, with mean δ^{34}S=4.8±0.7‰ Bao et al., 2007; see Fig. S3). The δ^{34}S and δ^{18}O show a weak, positive correlation (slope=0.2857, R^2=0.35; see Fig. S7). A Shapiro-Wilk test does not reject the null hypothesis that the data represent a normally distributed population (p-value=0.09).

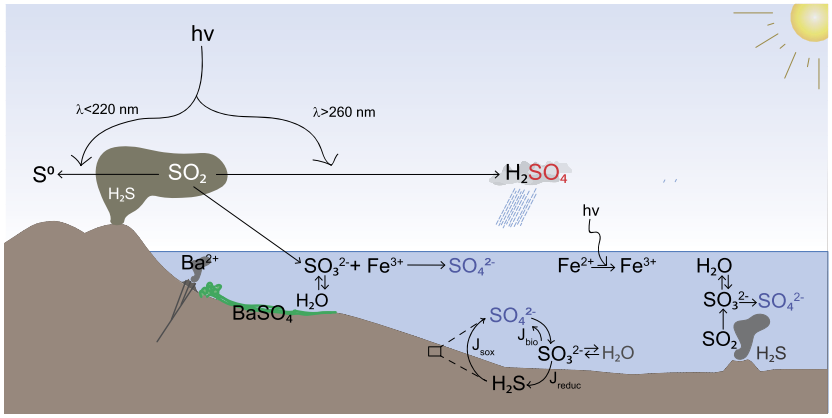

Fig. 2. Schematic diagram of the sources of sulfate to the Archean marine reservoir. Atmospheric sulfate (red) is thought to be the primary source of the positive $\Delta'^{17}O$ (mass-independent) signal measured in the triple oxygen isotope composition of the Fig Tree Group barite. Sulfate formed via other mechanisms (blue), during microbial sulfur cycling or the abiotic oxidation of sulfite, carries a mass-dependent signature. Double arrows represent oxygen isotope exchange. The terms J_{sox}, J_{bio}, and J_{reduc} represent the proportion of sulfate produced via microbial sulfide oxidation (sox) and microbial sulfate reduction (MSR; bio), versus the proportion reduced during MSR (reduc).

6. Discussion

Understanding the $\delta^{18}O$ of the Archean ocean is of central importance in diagnosing the interactions between seawater and the Archean lithosphere and biosphere. The triple oxygen isotope composition of barite offers a new way to constrain this composition. Extracting information about the contemporaneous ocean-atmosphere system from the data presented here requires that we first define an Archean sulfur cycle and the sources of sulfate to the Fig Tree Group barite. Here, we use a simple Monte Carlo approach to constrain the possible oxygen isotope composition of ambient seawater and to determine the magnitude of the relative contributions to seawater sulfate. We interpret the results of these exercises to gain insight into the composition of sulfate formed in the Archean atmosphere as well as the oxygen isotope composition of Archean seawater.

6.1. Sources of sulfate to the Fig Tree Group barite

The sulfate captured by the Fig Tree Group barite could be derived from a number of different sources. The sediments that host the barite deposits suggest a shallow marine to marginal terrestrial environment (a fan delta) (Drabon et al., 2019; Lowe et al., 2019), allowing for sulfate to be sourced from all major reservoirs (marine, terrestrial, atmospheric). The association of the barite deposits with vent structures suggests that barium-rich fluids were periodically injected into a sulfate-bearing surface water reservoir, rather than vice versa. The scale of these deposits (decimeter-scale thickness, tens of meters of lateral continuity) also requires a significant molar volume of sulfate over the lifetime of the vent to sustain barite production. As noted above, a marginal marine environment allows for the episodic contribution of seawater sulfate (understood to be at low concentrations in the Archean; e.g. Halevy, 2013) as well as sulfate derived from other anoxic oxidation pathways.

Before constructing a model of the Archean sulfur cycle, we first detail what we know about the modern sulfur cycle. In modern marine basins, the dominant input flux of sulfate is from rivers and is sourced from the oxidative weathering of terrestrial sulfide minerals and the dissolution of sulfate-bearing evaporites. The oxygen isotope composition of the resulting basinal sulfate is dependent on the magnitude and composition of this riverine sulfate and the net biological sulfate recycling flux (J_{bio}; see Fig. 2; Waldeck et al., 2019). Sulfate concentrations in modern rivers vary from ~1 mmol to ~100 µmol, depending on the prevalence of black shales (and thus sulfide minerals) and sulfate-bearing evaporites in the watershed (Hemingway et al., 2020). Additional fluxes, such as the atmospheric deposition of sulfate, are considered negligible in modern environments given a small relative contribution (Waldeck et al., 2019). However, prior to the Great Oxidation Event (GOE; ~2.4 Ga), Earth's atmospheric O_2 content likely did not exceed 10^{-5} of present atmospheric levels (PAL; Pavlov and Kasting, 2002). Widespread atmospheric and marine anoxia and the modest continental exposure proposed for the Archean both suggest minimal oxidative weathering (e.g., Halevy, 2013). As a result, estimates for Archean seawater sulfate concentrations are on the order of ~2.5 to ~200 μM (Jamieson et al., 2013; Halevy, 2013; Crowe et al., 2014), or a factor of 1000X less than today. A smaller global sulfate budget clearly carries consequences for the role of biology, but also the leverage atmospheric deposition could have.

In the Archean, most of the sulfur reaching the Earth's ocean-atmosphere system is likely sourced from volcanic outgassing of sulfur-bearing gases (H_2S and SO_2; Pavlov and Kasting, 2002; Halevy, 2013). These sulfur-bearing gasses could then be oxidized to sulfate via three main pathways: 1) as the result of photochemical reactions in the atmosphere (via the interaction of sulfur-bearing gases with HO_x species; e.g., Savarino et al., 2000), 2) abiotic reactions in the ocean (using an electron acceptor like Fe^{3+}), or 3) intra- or extracellular microbial sulfur cycling. In addition, the temporal and physical proximity of the Fig Tree Group barite deposits to impact-derived spherule beds also requires that we consider possible contributions from meteorites — a mechanism that has also been considered as the delivery mechanism for prebiotic molecules and as the enrichment mechanism for critical greenhouse gases (Kasting, 2014; Zherebker et al., 2021). Below, we consider the possible importance of each of these pathways.

We first consider the possibility that some or all of the sulfate delivered to the Fig Tree Group barite depocenter was meteorite-derived. We entertain this option despite the fact that detailed stratigraphic studies have found no link between the structures associated with the upper barite unit sampled from Eastern Barite Valley and any meteorite impact (Drabon et al., 2019; Lowe, 2013; Lowe et al., 2019). Sulfate bound in meteorites clearly carries a non-terrestrial origin. This sulfate carries a range of sulfur isotope compositions: $\delta^{34}S$=-1.15±1.48‰, $\Delta^{33}S$=+0.036±0.084‰, and $\Delta^{36}S$=-0.16±0.15‰ (n=13; Labidi et al., 2017; see SI Fig. S3 for a graphical illustration of the various sulfur pools found in Barite Valley). In contrast, the Fig Tree Group barite has a sulfur isotope composition of $\delta^{34}S$=+4.8±0.7‰, $\Delta^{33}S$=-0.55±0.11‰, and $\Delta^{36}S$=+1.9±1.6‰ (n=19, 14, and 12, respectively; Bao et al., 2007, with similar values measured in Roerdink et al., 2012), markedly different from extraterrestrial sulfate. The S2 and S3 spherule lay-

ers found in Barite Valley contain sulfide minerals that have $\delta^{34}S$=-1±1‰, $\Delta^{33}S$=0.80±0.02‰ and $\delta^{34}S$=2±2‰, $\Delta^{33}S$=0.7±0.5‰, respectively van Zuilen et al. (2014), making these unlikely sources of sulfur to the more oxidized sulfate pool.[1] Further, though separated in time, space, and perhaps depositional environment (Caruso et al., 2021), the 3.49 Ga Dresser Formation barite in Australia has a sulfur isotope composition similar to the Fig Tree Group barite, though with an even more depleted $\Delta^{33}S$ signature (<-1‰; Ueno et al., 2008; Bao et al., 2007). Despite evidence for multiple impacts in the Fig Tree Group (Lowe, 2013), the similarity between the Fig Tree Group and Dresser Formation sulfate pools may be evidence for a consistent Archean sulfate formation and delivery mechanism, neither of which require a significant extraterrestrial flux.

In contrast, the delivery of mantle-derived sulfur species to surface environments would have provided a persistant flux of sulfur throughout the Archean. The subsequent oxidation of this material could then serve as a plausible source of sulfate to the Archean ocean. Volcanic SO_2 and H_2S released into the anoxic Archean atmosphere would have experienced one of three possible fates: 1.) reduction (eventually to elemental sulfur), 2.) photolytic oxidation (eventually to H_2SO_4), or 3.) direct partitioning into seawater. Reduced sulfur species would have a short lifetime in seawater, reacting rapidly with readily available iron to form sulfide minerals (e.g., FeS_2). As such, reduced sulfur phases are not considered in our oxygen isotope budget. Volcanic SO_2 released during subaerial and submarine volcanism will partition into seawater as HSO_3^- (Halevy, 2013). The oxidation of sulfur-bearing gases would have been dependent on numerous variables, including the available wavelengths of radiation, the partial pressure of sulfur-bearing gasses (namely SO_2, H_2S), and features like the supply of atmospheric oxidants (OH, H_2O_2, etc.) in the Archean atmosphere (Halevy, 2013; Whitehill et al., 2015; Ono et al., 2013). In each case, the exact oxidation pathway to sulfate and the associated isotopic consequences are uncertain. Given that none of these variables are well known, we begin by dividing the oxidation pathways into two broad categories: marine (both abiotic and biotic) and non-marine (here, primarily considering atmospheric reactions).

Beginning in the ocean, the primary sulfur oxidation pathways available in Archean seawater were most likely either via the abiotic oxidation of sulfite by Fe^{3+} or through microbial sulfur cycling (e.g., Halevy, 2013). Importantly, the precursor to SO_4^{2-} during oxidation in an aqueous environment is sulfite (here meaning any sulfur species at oxidation state S(+IV)), which rapidly exchanges oxygen atoms with local waters (Bertran et al., 2020; Mizutani and Rafter, 1973; Wankel et al., 2014). Another possible source of sulfate to the barite is via the disproportionation of volcanic SO_2 supplied by local hydrothermal fluids (i.e., the vents; Kusakabe et al., 2000). At high temperatures (>150°C), SO_2 disproportionation can produce multiple sulfur species: S^0, H_2S, SO_3^{2-} or $S_2O_3^{2-}$, HSO_3^-, and HSO_4^- (Kusakabe et al., 2000). Intermediate-valence sulfoxy anions such as SO_3^{2-} (sulfite) or $S_2O_3^{2-}$ (thiosulfate) that escaped terminal reduction and sequestration could have been oxidized to the more stable SO_4^{2-} by Fe^{3+} (Halevy, 2013), recording at least a partial equilibrium with seawater.[2] Biological oxidation would also pass through this same set of intermediate-valence sulfoxy anions. Further, during microbial sulfate reduction (MSR), there is a significant efflux of sulfate from the cell with a new, reset oxygen isotope composition (Farquhar et al., 2008). This is sulfate that was taken up, partially reduced, reoxidized within the cell, and which escapes terminal reduction to H_2S (Farquhar et al., 2008). This effluxed sulfate is isotopically equilibrated with ambient water during an intermediate sulfite step (Bertran et al., 2020). In addition, modeling suggests that the seawater sulfate reservoir was isotopically well-mixed, connecting shallower depositional environments to the broader Archean ocean (Halevy, 2013). In sum, the resulting seawater sulfate reservoir that could contribute to the Fig Tree Group barite will carry a component that was equilibrated with seawater during sulfate generation and potentially contain information about specific sulfur oxidation pathways (i.e., Fe^{3+} oxidation or MSR).

The final consideration for sulfate generation is through atmospheric deposition. We differentiate sulfuric acid rain (our atmospheric component) from sulfur-bearing gasses partitioning into seawater given the location of oxidation (the atmosphere) and the associated suite of possible oxidants (HO_x, etc.). However, placing unique isotopic constraints on atmospheric sulfate is much more challenging than in the aqueous oxidation scenarios outlined above. For this reason, we stop short of making specific claims and rely on modelling predictions to assign this sulfate a possible isotopic composition (see below).

6.2. Constraining the oxygen isotope composition of Archean seawater sulfate

The oxygen isotope composition of the Fig Tree barite likely carries information about the source of that sulfate. Accordingly, the isotopic composition of the barite can be described via a mixing relationship that reflects the probable sources of sulfate eventually captured by the barite deposits. This can be expressed as:

$$\delta^{1X}O_{sulfate} = J_{bio} * \delta^{1X}O_{bio} + J_{abio} * \delta^{1X}O_{abio} + J_{atm} * \delta^{1X}O_{atm}, \quad (6)$$

where ^{1X}O is either ^{17}O or ^{18}O and J is the relative contribution of each input at steady-state (J_{atm}+J_{bio}+J_{abio}=1). The term J_{atm} is defined as the relative contribution of 'atmospheric sulfate', and is irrespective of the specific oxidation mechanism. The remaining terms, J_{bio} and J_{abio}, are the relative contributions of sulfate formed via the oxidation of more reduced sulfur species via the sulfite anion, resulting in some expression of an isotopic equilibrium with ambient seawater at that stage in the oxidation reaction. Here, J_{bio} is illustrated in Fig. 2 as the contribution of sulfate that has been recycled and equilibrated with water via a microbial metabolism, while J_{abio} represents the sulfur that has been oxidized to sulfate via abiotic pathways using an oxidant like Fe^{3+}. Below, we simplify this equation and focus on each endmember in turn to reconstruct an Archean sulfate budget.[3]

Though the exact triple oxygen isotope effect of J_{bio} and J_{abio} is under-constrained, we can conservatively estimate the likely endmember oxygen isotope compositions possible for both of these marine oxidation pathways. To capture the possible range of compositions derived from both J_{bio} and J_{abio}, we employ a simple inverse Monte Carlo sampling approach (see SI for further detail). The output of this exercise is a family of predictions for the oxygen isotope composition of the ambient water within which each of these reaction pathways occur (i.e., seawater, basinal water, etc.).

[1] The S2 spherule deposit is stratigraphically below the barite deposits in both Eastern and Western Barite Valley, while the S3 spherule deposit is found below the barite in Eastern Barite Valley and within the Western Barite Valley barite horizons.

[2] Sulfate formed directly from magmatic SO_2 disproportionation should carry juvenile sulfur compositions and have $\delta^{34}S$ values uniformly >15‰ more enriched than co-occurring sulfide minerals (Kusakabe et al., 2000), which is not observed in the Barite Valley deposits (Roerdink et al., 2013; Bao et al., 2007), we thus do not consider a significant flux of magmatic SO_2.

[3] Diagnosing differential contributions to sulfate via mass-balance accounting can also be done for sulfur. However, that approach does not offer any added insight in this particular exercise and is therefore excluded.

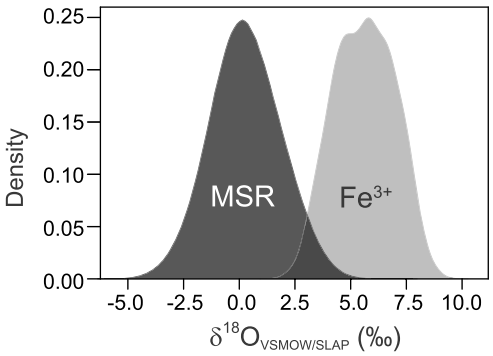

Fig. 3. Estimates of the oxygen isotope composition of Archean seawater from a Monte Carlo simulation of two mass-dependent oxidation pathways: abiotic oxidation via Fe^{3+} and microbial sulfur cycling (MSR).

As an input, this inverse approach uses the $\delta^{18}O$ composition of the Fig Tree Group barite presented in this study, in conjunction with previously published data (Bao et al., 2007; recalibrated to reflect different data acquisition techniques; Waldeck, 2021). Further, both of these potential fluxes are related to the oxygen isotope composition of water via the temperature-dependent abiotic equilibration of SO_3^{2-} with H_2O:

$$\epsilon_{SO3-H2O} = 13.61 - 0.299 * pH - 0.081 * T, \quad (7)$$

where T is in °C (Wankel et al., 2014). From here, for the purposes of this calculation, we assume the extreme cases where each oxidation pathway — Fe^{3+} and MSR — account for 100% of the sulfate captured by the Fig Tree Group barite. In other words, we simplify the mixing equation presented above by setting J_{atm} to 0 and J_{abio} or J_{bio} to 1. For J_{abio}, the subsequent oxidation of equilibrated SO_3^{2-} to SO_4^{2-} via Fe^{3+} in an anoxic environment imposes an additional 5.8±0.7‰ isotope effect (Müller et al., 2013). For J_{bio}, the effect is more variable, but in general, it is thought that modern metabolisms cause an isotope effect (ϵ_{bio}) between H_2O and SO_4^{2-} of ~25‰ during MSR (Bertran et al., 2020). At Archean-like sulfate and sulfide concentrations, this effect becomes more variable and closer to ~10‰ (holding reduction rates constant; Bertran et al., 2020). With this in mind, our Monte Carlo approach samples from a uniform distribution of conservative Archean water temperatures (0-50°C; Krissansen-Totton et al., 2018) and pH values (6.4-7.4; Halevy and Bachan, 2017; Catling and Zahnle, 2020) for each iteration (Table S2). The result is a family of solutions for the possible composition of Archean seawater. Though the oxygen isotope composition of the basin water would largely be set by the global ocean, we do acknowledge possible deviation from this composition due to basin restriction/evolution (Waldeck et al., 2022) or meteoric inputs in a marginal marine environment, which are discussed more below. Since each of these processes can drive the oxygen isotope composition of water in opposite directions, we further stress the 'estimate' aspect of this work and look to further geological and geochemical observations to help provide clarity. Caveats aside, using the isotope effects predicted for either Fe^{3+} oxidation or MSR in Archean seawater (10±2‰; Bertran et al., 2020) yields predictions for early Archean seawater with $\delta^{18}O$=5.6±1.4‰ and $\delta^{18}O$=0.3±2.3‰, respectively (Fig. 3), in agreement with recent models that similarly predict an ^{18}O-enriched Archean ocean (e.g., Sukanya Sengupta and Peter, 2020; Johnson and Wing, 2020).

We can take an even more conservative approach and run this Monte Carlo simulation in reverse, as well. If we assume that the oxygen isotope composition of Archean seawater was between -14 and +3.3‰ (Jaffrés et al., 2007; Johnson and Wing, 2020), then using the same mass-dependent pathways described above, we can

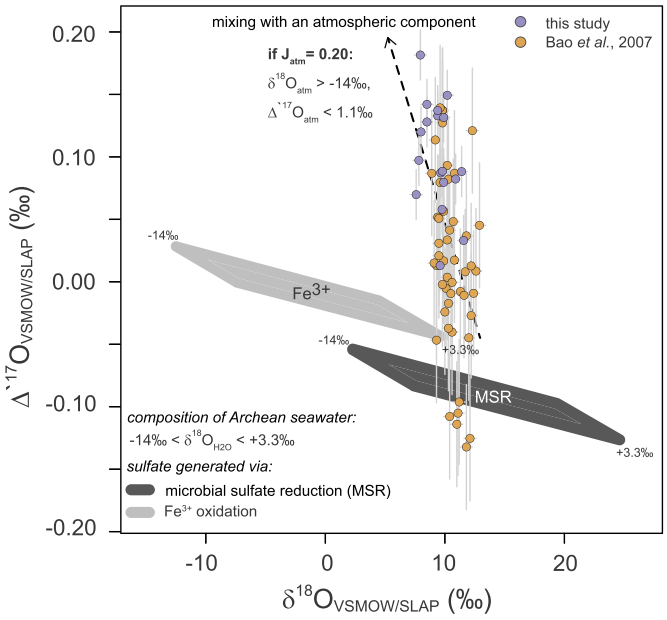

Fig. 4. Estimates of the oxygen isotope composition of Archean seawater sulfate from a Monte Carlo simulation of two mass-dependent oxidation pathways: abiotic oxidation via Fe^{3+} (light grey envelope) and microbial sulfur cycling (MSR; dark grey envelope). The sulfate compositions are calculated using the full range of reported oxygen isotope compositions for Archean seawater (-14‰ Jaffrés et al., 2007 to +3.3‰ Johnson and Wing, 2020; see SI for more details on the model parameters). The dashed line represents a linear regression through the data and the line that best represents mixing between seawater sulfate and atmospheric sulfate.

predict the triple oxygen isotope composition of the sulfate formed by a given pathway (Fig. 4). Those predictions for Archean sulfate can then be compared to the composition of the Fig Tree Group barite. We presume mass-dependence and use a mass-law of θ=0.5250 for both pathways along with the presumption that a starting water composition would fall along the meteoric water line (MWL) with θ=0.5280 (Hemingway et al., 2022; Sharp et al., 2018). The addition of meteoric water to the basin would extend the mass-dependent envelopes drawn in Fig. 4 towards more positive $\Delta'^{17}O$ and more negative $\delta^{18}O$ compositions. The assumption of mass-dependence for both these oxidation mechanisms should be tested, but is very likely. Alternative θ values will only modestly change these results (slightly changing the slope of the envelopes presented in Fig. 4), especially in comparison to the range of compositions represented in the Fig Tree Group. To illustrate the maximal possible range of sulfate compositions, we use the full expression of the isotope effect predicted for MSR (ϵ_{bio}=25‰), though this is likely an overestimate given the low concentration of sulfate and sulfide in the Archean ocean Bertran et al., 2020). As such, smaller isotope effects would cause the J_{bio} to shrink to cover a smaller range (linearly with the size of the assigned ϵ).

In both approaches noted above, oxygen isotope arguments constrain the two marine oxidation pathways as if they each represented 100% of the sulfate captured in these deposits (J=1). These results suggest that the oxygen isotope composition of Archean seawater would be enriched if the majority of the sulfate is supplied via Fe^{3+}-oxidation (Figs. 3 and 4). These predictions become more depleted if the majority of sulfate is the result of cellular efflux during MSR, with the composition varying between ~0‰ and -15‰, depending on the sulfate and sulfide concentrations and reduction rates (Bertran et al., 2020).

In fact, there are multiple lines of evidence that point to a muted biogeochemical sulfur cycle (low J_{bio}). Here, we can call on the sulfur isotope data for more insight. First, a significant MSR component would be expected to produce a correspondingly significant amount of sulfide (H_2S), which would immediately be

sequestered as pyrite via the reaction with Fe^{2+} in the ferruginous Archean ocean. The disseminated pyrite that is found within the Fig Tree Group barite has been interpreted as the result of MSR (Roerdink et al., 2012), showing that there is, indeed a non-zero J_{bio} contribution. This is the mass-dependent translation of mass-independent sulfur from sulfate to sulfide and hence carries a mass-balance requirement. However, significant sulfide mineral deposits are not observed in the Fig Tree Group barite (Lowe et al., 2019). Any sulfate reduction would also drive the residual sulfate towards more enriched and variable $\delta^{34}S$ compositions, which is not seen in the relatively uniform composition of the Fig Tree Group barite ($\delta^{34}S$=+4.1±0.6‰, n=17). Further, the preservation of a mass-independent $\Delta'^{17}O$ composition in the barite precludes complete resetting by microbes (Bao et al., 2007; Halevy et al., 2010). A significant mass-dependent component, buffered by a near infinite reservoir of water oxygen, would erase these mass-independent signatures. Therefore, J_{bio} is likely relatively insignificant in setting the oxygen isotopes of sulfate in the Fig Tree Group barite. If true, this leaves J_{abio} as the likely dominant mass-dependent component, which does not accommodate a depleted isotopic composition for the Archean ocean and instead suggests a composition that may have even exceeded >+3.3‰ at 3.2 Ga (in agreement with Johnson and Wing, 2020). This interpretation would also be incompatible with a significant contribution from depleted meteoric waters (Fig. 4). Of course, the exact oxygen isotope composition of the water depends on the proportion of the J_{bio} to J_{abio} as well as the flux of atmospheric sulfate.

6.3. The oxygen isotope composition of Archean atmospheric sulfate

The arguments above shed new light onto the possible composition of Archean seawater and on the relative importance of an early microbial sulfur cycle. However, it is also clear from the mismatch between these predictions and the triple oxygen isotope composition of Fig Tree Group barite — most prominently captured in the $\Delta'^{17}O$ composition — that an additional sulfate source is needed to satisfy the data (Fig. 4). Note that the data-model mismatch considers J_{bio} and J_{abio}. If our mixing model is appropriate, then the apparent 'mismatch' is telling us something about J_{atm}, the final component in the overall mass balance. Further, given the steep slope of the $\delta^{18}O$ - $\Delta'^{17}O$ (θ=0.4998), it is possible and perhaps even likely that the reactions forming sulfate in the atmosphere are either mass-independent, or sample an oxidant reservoir that is itself subject to mass-independent chemistry. If, in fact, Fig Tree Group barite represents a mixture of mass-dependent (J_{bio} and J_{abio}) processes residing within the model predictions in Fig. 4, and mass-independent sulfate (from J_{atm}), as is likely the case (Halevy, 2013), then an estimate can be placed on the composition of the pure photochemical end-member.

At first pass, photochemically derived sulfate in the Archean would have had a $\delta^{18}O$<10.3‰ and $\Delta'^{17}O$>+0.038 (the average composition of the Fig Tree Group barite). It is possible that oxidation of atmospheric SO_2 accounted for more than 20% of the sulfate in the Archean ocean (Halevy, 2013). If we assume that this sulfate carried a positive $\Delta'^{17}O$, explaining the deviation from mass-dependence of the data, then the composition of this sulfate must be less than or equal to the most depleted $\delta^{18}O$ composition (7.6‰) and greater than or equal to the most enriched $\Delta'^{17}O$ composition (+0.18‰) of the measured sulfate. For illustration purposes, we can also treat the data as the result of mixing between sulfate formed in the atmosphere and sulfate (a joint J_{bio} - J_{abio} endmember) formed in the water column. Here we fix the J_{bio} - J_{abio} endmember composition at $\delta^{18}O$=13‰ and $\Delta'^{17}O$=-0.05‰ — the approximate value where the data array intersects model predictions). If, for a moment, we consider a minimum 20% contribution from atmospheric sulfate (J_{atm}=0.20; Halevy, 2013), then the prediction for the isotopic composition of the atmospheric endmember would be at least $\delta^{18}O$=-14‰ with a corresponding $\Delta'^{17}O$ composition of at most +1.1‰ (see SI for further discussion of the full range in composition). Importantly, this prediction would require a *mass-independent* oxidation mechanism or contributions from a mass-indepedent oxidant. In the modern, mass-independent oxygen isotope effects are generated via the interaction between atmospheric O_3, O_2, and CO_2, reactions unlikely in an anoxic Archean atmosphere (e.g., Cao and Bao, 2013).

Returning to the modern, the generation of mass-independent oxygen isotope effects are the result of both a suite of photochemical reactions involving oxygen-bearing species (e.g., Cao and Bao, 2013; Thiemens, 2006; Heinrichs and Reimer, 1977) and the resulting mass-balance between species. The same framework would apply in the Archean, although with different chemistry, overall mass-balance, and mechanism of transferring this signal to sulfate. One could envision that the magnitude and sign of the sulfate-generating reactions are dependent on the identity, residence time, and partial pressure of the available oxidant (O_2, H_2O_2, etc.; Cao and Bao, 2013; Savarino et al., 2000). For example, H_2O_2 can be generated from photochemical reactions involving H_2O in a low-O_2 atmosphere, but only has a lifetime on the order of hours (Liang et al., 2006). This would suggest a limited opportunity for photochemical H_2O_2 to encounter an S-bearing phase, before even considering the sheer scale of oxidizing capacity needed to (locally) generate the sulfate captured by the Fig Tree Group barite. Other mechanisms for incorporating a photochemical signal are similarly opaque. For instance, laboratory experiments where SO_2 is reacted with OH or H_2O to generate sulfate both generate mass-dependent sulfate (and have only been constrained in the presence of O_2; Savarino et al., 2000). There is a mass-independent signal produced as the result of the photodissociation of pure CO (Chakraborty et al., 2012), but the translation of this signal to an Archean atmosphere (with higher relative pCO_2) and ultimately to sulfate remains unclear. So, while we cannot identify the exact mechanism or oxidant that is imparting a potential mass-independent signal to Archean atmospheric sulfate, we can offer empirical and mass-balance constraints.

One distant example of the oxygen isotope composition of sulfate generated in an anoxic atmosphere might come from Mars. Interestingly, the composition of sulfate measured in the Martian Nakhla meteorite is similar to the atmospheric sulfate endmember that we propose above. At J_{atm}=0.2, atmospheric sulfate has a positive $\Delta'^{17}O$ signal (<1.1‰) and likely a negative $\delta^{18}O$ signal (>-14‰), dependent of course on the size of the atmospheric component. Intriguingly, water soluble sulfate from Nakhla has $\delta^{18}O$=-3.72‰ and $\Delta'^{17}O$=+1.37‰ (θ=0.5305 Farquhar and Thiemens, 2000). This sulfate has been proposed to form in the Martian atmosphere via oxidation by H_2O_2, O_3, or the photolysis of SO_2 (Farquhar and Thiemens, 2000). A positive $\Delta'^{17}O$ signal of this magnitude requires sequestration of a negative signal into another oxygen-bearing species. We do not see a significant negative mass-independent signal in Archean clays or silicates (e.g., Lowe et al., 2020; Liljestrand et al., 2020; Sukanya Sengupta and Peter, 2020), indicating that this signal may be effectively erased via incorporation into Archean seawater. Regardless, the similarity between Martian and Archean atmospheric sulfate requires the presence of a significant pool of an atmospheric oxidant with a positive $\Delta'^{17}O$ in both planetary atmospheres and could implicate that ozone photochemistry was important long before the Great Oxidation Event.

While the atmospheric component remains underconstrained, we gain insight into the joint J_{bio} and J_{abio} endmember compositions. If this interpretation is correct, then the relative dominance of J_{abio} over J_{bio} exerts the primary control on the $\delta^{18}O$ of Archean seawater. If we presume a small J_{bio} from sulfur isotope

studies, then J_{abio} controls aqueous oxidative pathways and estimates for the isotope composition of Archean seawater are likely more similar to +3.3 ‰ (Johnson and Wing, 2020). This would be inconsistent with a highly depleted seawater in the Archean ocean (-14‰ or -10‰; Jaffrés et al., 2007; Kasting et al., 2006) or with a basin dominated by isotopically depleted meteoric waters. Thus, these results may point to either elevated SSTs (Lowe et al., 2020) or to diagenetic alteration (Liljestrand et al., 2020) as an explanation for the apparent oxygen isotope depletion in Archean chemical sediments. Though this sample set represents only a single time point in the Archean, the Fig Tree Group barite may support a somewhat invariant oxygen isotope composition of seawater throughout geologic time.

7. Conclusions

The geological record offers only a fleeting glimpse of the Archean sulfate budget, with one of the central archives being the Fig Tree Group barite. These marginal marine deposits preserve a tight relationship between $\delta^{18}O$ and $\Delta'^{17}O$ — a composition that can be understood by examining the various reaction pathways (inorganic, microbial and photochemical) for sulfate generation in an anoxic Archean world. It is not possible to uniquely determine the magnitude and isotopic signature of each of these fluxes, but some key conclusions are indeed possible. First, essentially regardless of the magnitude of photochemical sulfate delivery to the ocean, the $\delta^{18}O$ of that sulfate must have been <10.3‰ with a $\Delta'^{17}O$ >+0.038‰. If independent photochemical estimates are used Halevy (2013), then this sulfate carries a composition closer to $\delta^{18}O$=-14‰ and $\Delta'^{17}O$=+1.1‰, which is similar to the oxygen isotope composition of sulfate proposed to have formed in the Martian atmosphere. This parallel suggests there may be a common oxidation mechanism occurring in both planetary atmospheres. We also interpret these data to suggest that microbial sulfur cycling was not vigorous, as sulfate recycling through microbial metabolisms would bring atmospheric sulfate into equilibrium with seawater. Further, vigorous MSR is inconsistent with both the lack of co-occurring pyrite and the sulfur isotope signature of the Fig Tree Group barite. These conclusions suggest that sulfate in the Archean ocean was largely sourced from abiotic oxidation in seawater, with lesser fluxes from both photochemical oxidation in the atmosphere and microbial sulfur cycling. If true, then the isotopic composition of the Archean ocean was likely somewhat enriched in ^{18}O, with a slightly depleted $\Delta'^{17}O$ composition. This conclusion provides more evidence that low-temperature interactions between seawater and oceanic crust were less important earlier in Earth history, perhaps supporting the idea of an Archean "water world" (Johnson and Wing, 2020; Sukanya Sengupta and Peter, 2020).

CRediT authorship contribution statement

Haley C. Olson: Conceptualization, Formal analysis, Investigation, Methodology, Writing – original draft. **Nadja Drabon:** Writing – original draft. **David T. Johnston:** Conceptualization, Formal analysis, Funding acquisition, Investigation, Methodology, Resources, Writing – original draft.

Declaration of competing interest

The authors declare that they have no known competing financial interests or personal relationships that could have appeared to influence the work reported in this paper.

Acknowledgements

We thank all members of the Johnston group for their advice on the technical aspects of the paper as well as for detailed feedback and discussions which improved the manuscript. We also thank Emily Stoll for help collecting the barite samples. Additionally, we thank Peter Ryan at Middlebury College for the XRD data he provided and the Gill Lab at Virgina Tech for sulfur isotope measurements. We are grateful for detailed feedback from the editor (Dr. Boswell Wing) and two reviewers (Dr. Christoph Heubeck and one anonymous reviewer), which greatly improved the manuscript. Sappi allowed us access to their private plantation property. Funding for this work was provided by Harvard University (H.O.) and NSF OCE-1821958 and NSF OCE-1946137 (D.J.).

Appendix A. Supplementary material

Supplementary material related to this article can be found online at https://doi.org/10.1016/j.epsl.2022.117603.

References

Bao, H., Rumble, D., Lowe, D.R., 2007. The five stable isotope compositions of Fig Tree barites: implications on sulfur cycle in ca. 3.2 Ga oceans. Geochim. Cosmochim. Acta 71 (20), 4868–4879.
Bao, H., Lyons, J., Zhou, C., 2008. Triple oxygen isotope evidence for elevated CO_2 levels after a Neoproterozoic glaciation. Nature 453 (7194), 504–506.
Bao, H., Cao, X., Hayles, J.A., 2016. Triple oxygen isotopes: fundamental relationships and applications. Annu. Rev. Earth Planet. Sci. 44, 463–492.
Bertran, E., Waldeck, A., Wing, B., Halevy, I., Leavitt, W., Bradley, A., Johnston, D., 2020. Oxygen isotope effects during microbial sulfate reduction: applications to sediment cell abundances. ISME J. 14, 1508–1519.
Bindeman, I.N., Bayon, G., Palandri, J., 2019. Triple oxygen isotope investigation of fine-grained sediments from major world's rivers: insights into weathering processes and global fluxes into the hydrosphere. Earth Planet. Sci. Lett. 528, 115851.
Blake, R.E., Chang, S.J., Lepland, A., 2010. Phosphate oxygen isotopic evidence for a temperate and biologically active Archaean ocean. Nature 464 (7291), 1029–1032.
Byerly, G.R., Kröner, A., Lowe, D.R., Todt, W., Walsh, M.M., 1996. Prolonged magmatism and time constraints for sediment deposition in the early Archean Barberton Greenstone Belt: evidence from the Upper Onverwacht and Fig Tree Groups. Precambrian Res. 78 (1), 125–138.
Cao, X., Bao, H., 2013. Dynamic model constraints on oxygen-17 depletion in atmospheric $_2$ after a snowball Earth. Proc. Natl. Acad. Sci. 110 (36), 14546–14550.
Cao, X., Liu, Y., 2011. Equilibrium mass-dependent fractionation relationships for triple oxygen isotopes. Geochim. Cosmochim. Acta 75 (23), 7435–7445.
Caruso, S., Van Kranendonk, M.J., Baumgartner, R.J., Fiorentini, M.L., Forster, M.A., 2021. The role of magmatic fluids in the ~3.48 Ga Dresser Caldera, Pilbara Craton: new insights from the geochemical investigation of hydrothermal alteration. Precambrian Res. 362, 106299.
Catling, D.C., Zahnle, K.J., 2020. The Archean atmosphere. Sci. Adv. 6 (9).
Chakraborty, S., Davis, R.D., Ahmed, M., Jackson, T.L., Thiemens, M.H., 2012. Oxygen isotope fractionation in the vacuum ultraviolet photodissociation of carbon monoxide: wavelength, pressure, and temperature dependency. J. Chem. Phys. 137 (2).
Claypool, G.E., Holser, W.T., Kaplan, I.R., Sakai, H., Zak, I., 1980. The age curves of sulfur and oxygen isotopes in marine sulfate and their mutual interpretation. Chem. Geol. 28, 199–260.
Cowie, B.R., Johnston, D.T., 2016. High-precision measurement and standard calibration of triple oxygen isotopic compositions (δ18O, Δ'17O) of sulfate by F2 laser fluorination. Chem. Geol. 440, 50–59.
Crockford, P.W., Hayles, J.A., Bao, H., Planavsky, N.J., Bekker, A., Fralick, P.W., Halverson, G.P., Bui, T.H., Peng, Y., Wing, B.A., 2018. Triple oxygen isotope evidence for limited mid-Proterozoic primary productivity. Nature 559 (7715), 613–616.
Crowe, S.A., Paris, G., Katsev, S., Jones, C.A., Kim, S.T., Zerkle, A.L., Nomosatryo, S., Fowle, D.A., Adkins, J.F., Sessions, A.L., Farquhar, J., Canfield, D.E., 2014. Sulfate was a trace constituent of Archean seawater. Science 346 (6210), 735–739.
Drabon, N., Lowe, D.R., 2021. Progressive accretion recorded in sedimentary rocks of the 3.28–3.23 ga Fig Tree group, Barberton Greenstone Belt. Geol. Soc. Am. Bull. 72 (0016–7606), 1–19.
Drabon, N., Heubeck, C.E., Lowe, D.R., 2019. Evolution of an Archean fan delta and its implications for the initiation of uplift and deformation in the Barberton Greenstone Belt, South Africa. J. Sediment. Res. 89 (9), 849–874.
Farquhar, J., Thiemens, M.H., 2000. Oxygen cycle of the Martian atmosphere-regolith system: $\Delta^{17}O$ secondary phases in Nakhla and Lafayette. J. Geophys. Res. 105 (E5), 11991–11997.

Farquhar, J., Bao, H., Thiemens, M., 2000. Atmospheric influence of Earth's earliest sulfur cycle. Science 289 (5480), 756–758.
Farquhar, J., Canfield, D.E., Masterson, A., Bao, H., Johnston, D., 2008. Sulfur and oxygen isotope study of sulfate reduction in experiments with natural populations from Fællestrand, Denmark. Geochim. Cosmochim. Acta 72 (12), 2805–2821.
Halevy, I., 2013. Production, preservation, and biological processing of mass-independent sulfur isotope fractionation in the Archean surface environment. Proc. Natl. Acad. Sci. 110 (44), 17644–17649.
Halevy, I., Bachan, A., 2017. The geologic history of seawater pH. Science 355 (6329), 1069–1071.
Halevy, I., Johnston, D.T., Schrag, D.P., 2010. Explaining the structure of the Archean mass-independent sulfur isotope record. Science 329, 204–208.
Heinrichs, T.K., Reimer, T., 1977. A sedimentary barite deposit from the Archean Fig Tree Group of the Barberton Mountain Land (South Africa). Econ. Geol., Bull. Soc. Econ. Geol. 72 (8), 1426–1441.
Hemingway, J.D., Olson, H., Turchyn, A.V., Tipper, E.T., Bickle, M.J., Johnston, D.T., 2020. Triple oxygen isotope insight into terrestrial pyrite oxidation. Proc. Natl. Acad. Sci. 117 (14), 7650–7657.
Hemingway, J.D., Goldberg, M.L., Sutherland, K.M., Johnston, D.T., 2022. Theoretical estimates of sulfoxyanion triple-oxygen equilibrium isotope effects and their implications. Geochim. Cosmochim. Acta. https://doi.org/10.1002/essoar.10508624.1.
Hodgskiss, M.S., Crockford, P.W., Peng, Y., Wing, B.A., Horner, T.J., 2019. A productivity collapse to end Earth's great oxidation. Proc. Natl. Acad. Sci. 116 (35), 17207–17212.
Holser, W.T., Kaplan, I.R., Sakai, H., Zak, I., 1979. Isotope geochemistry of oxygen in the sedimentary sulfate cycle. Chem. Geol. 25 (1–2), 1–17.
Jaffrés, J.B., Shields, G.A., Wallmann, K., 2007. The oxygen isotope evolution of seawater: a critical review of a long-standing controversy and an improved geological water cycle model for the past 3.4 billion years. Earth-Sci. Rev. 83 (1–2), 83–122.
Jamieson, J.W., Wing, B.A., Farquhar, J., Hannington, M.D., 2013. Neoarchaean seawater sulphate concentrations from sulphur isotopes in massive sulphide ore. Nat. Geosci. 6 (1), 61–64.
Johnson, B.W., Wing, B.A., 2020. Limited Archaean continental emergence reflected in an early Archaean ^{18}O-enriched ocean. Nat. Geosci. 13 (3), 243–248.
Kasting, J.F., 2014. Atmospheric composition of Hadean-early Archean Earth: the importance of CO. Spec. Pap., Geol. Soc. Am. 504 (04), 19–28.
Kasting, J.F., Howard, M.T., Wallmann, K., Veizer, J., Shields, G., Jaffrés, J., 2006. Paleoclimates, ocean depth, and the oxygen isotopic composition of seawater. Earth Planet. Sci. Lett. 252 (1), 82–93.
Knauth, L.P., Epstein, S., 1976. Hydrogen and oxygen isotope ratios in nodular and bedded cherts. Geochim. Cosmochim. Acta 40 (9), 1095–1108.
Krissansen-Totton, J., Arney, G.N., Catling, D.C., 2018. Constraining the climate and ocean pH of the early Earth with a geological carbon cycle model. Proc. Natl. Acad. Sci. 115 (16), 4105–4110.
Kusakabe, M., Komoda, Y., Takano, B., Abiko, T., 2000. Sulfur isotopic effects in the disproportionation reaction of sulfur dioxide in hydrothermal fluids: implications for the δ^{34}S variations of dissolved bisulfate and elemental sulfur from active crater lakes. J. Volcanol. Geotherm. Res. 97 (1), 287–307.
Labidi, J., Farquhar, J., Alexander, C., Eldridge, D., Oduro, H., 2017. Mass independent sulfur isotope signatures in CMs: implications for sulfur chemistry in the early solar system. Geochim. Cosmochim. Acta 196, 326–350.
Liang, M.-C., Hartman, H., Kopp, R.E., Kirschvink, J.L., Yung, Y.L., 2006. Production of hydrogen peroxide in the atmosphere of a Snowball Earth and the origin of oxygenic photosynthesis. Proc. Natl. Acad. Sci. 103 (50), 18896–18899.
Liljestrand, F.L., Knoll, A.H., Tosca, N.J., Cohen, P.A., Macdonald, F.A., Peng, Y., Johnston, D.T., 2020. The triple oxygen isotope composition of Precambrian chert. Earth Planet. Sci. Lett. 537, 116167.
Lloyd, R., 1968. Oxygen isotope behavior in the sulfate-water system. J. Geophys. Res. 73 (18), 6099–6110.
Lowe, D.R., 2013. Crustal fracturing and chert dike formation triggered by large meteorite impacts, ca. 3.260 Ga, Barberton Greenstone Belt, South Africa. Geol. Soc. Am. Bull. 125 (5–6), 894–912.
Lowe, D.R., Byerly, G.R., 1999. Stratigraphy of the west-central part of the Barberton Greenstone Belt, South Africa. Spec. Pap., Geol. Soc. Am. 329, 1–36.
Lowe, D.R., Drabon, N., Byerly, G.R., 2019. Crustal fracturing, unconformities, and barite deposition, 3.26–3.23 Ga, Barberton Greenstone Belt, South Africa. Precambrian Res. 327, 34–46.
Lowe, D.R., Ibarra, D.E., Drabon, N., Chamberlain, C.P., 2020. Constraints on surface temperature 3.4 billion years ago based on triple oxygen isotopes of cherts from the Barberton Greenstone Belt, South Africa, and the problem of sample collection. Am. J. Sci. 320 (9), 790–814.
Mizutani, Y., Rafter, T.A., 1973. Isotopic behaviour of sulphate oxygen in the bacterial reduction of sulphate. Geochem. J. 6 (4), 183–191.
Muehlenbachs, K., 1998. The oxygen isotopic composition of the oceans, sediments and the seafloor. Chem. Geol. 145 (3–4), 263–273.
Muller, Élodie, Philippot, P., Rollion-Bard, C., Cartigny, P., 2016. Multiple sulfur-isotope signatures in Archean sulfates and their implications for the chemistry and dynamics of the early atmosphere. Proc. Natl. Acad. Sci. 113 (27), 7432–7437.
Müller, I.A., Brunner, B., Coleman, M., 2013. Isotopic evidence of the pivotal role of sulfite oxidation in shaping the oxygen isotope signature of sulfate. Chem. Geol. 354, 186–202.
Ono, S., Whitehill, A.R., Lyons, J.R., 2013. Contribution of isotopologue self-shielding to sulfur mass-independent fractionation during sulfur dioxide photolysis. J. Geophys. Res. 118 (5), 2444–2454.
Pavlov, A.A., Kasting, J.F., 2002. Mass-independent fractionation of sulfur isotopes in Archean sediments: strong evidence for an anoxic Archean atmosphere. Astrobiology 2 (1), 27–41.
Roerdink, D.L., Mason, P.R., Farquhar, J., Reimer, T., 2012. Multiple sulfur isotopes in Paleoarchean barites identify an important role for microbial sulfate reduction in the early marine environment. Earth Planet. Sci. Lett. 331–332, 177–186.
Roerdink, D.L., Mason, P.R., Whitehouse, M.J., Reimer, T., 2013. High-resolution quadruple sulfur isotope analyses of 3.2 ga pyrite from the Barberton Greenstone Belt in South Africa reveal distinct environmental controls on sulfide isotopic arrays. Geochim. Cosmochim. Acta 117, 203–215.
Savarino, J., Lee, C.C.W., Thiemens, M.H., 2000. Laboratory oxygen isotopic study of sulfur (IV) oxidation: origin of the mass-independent oxygen isotopic anomaly in atmospheric sulfates and sulfate mineral deposits on Earth. J. Geophys. Res. 105.
Sharp, Z., Wostbrock, J., Pack, A., 2018. Mass-dependent triple oxygen isotope variations in terrestrial materials. Geochem. Perspect. Lett. 7, 27–31.
Sukanya Sengupta, J.R.J.-P.D., Peter, Stefan T.M., 2020. Triple oxygen isotopes of cherts through time. Chem. Geol. 554, 119789.
Thiemens, M.H., 2006. History and applications of mass-independent isotope effects. Annu. Rev. Earth Planet. Sci. 34, 217–262.
Ueno, Y., Ono, S., Rumble, D., Maruyama, S., 2008. Quadruple sulfur isotope analysis of ca. 3.5 Ga Dresser Formation: new evidence for microbial sulfate reduction in the early Archean. Geochim. Cosmochim. Acta 72 (23), 5675–5691.
Urey, H.C., 1947. Chemical properties of isotopic compounds. Chimia 1 (4), 90.
van Zuilen, M., Philippot, P., Whitehouse, M., Lepland, A., 2014. Sulfur isotope mass-independent fractionation in impact deposits of the 3.2 billion-year-old Mapepe Formation, Barberton Greenstone Belt, South Africa. Geochim. Cosmochim. Acta 142, 429–441.
Waldeck, A.R., 2021. Stable oxygen isotopes in sulfate: implications for Phanerozoic pO2. PhD Thesis.
Waldeck, A., Cowie, B., Bertran, E., Wing, B., Halevy, I., Johnston, D., 2019. Deciphering the atmospheric signal in marine sulfate oxygen isotope composition. Earth Planet. Sci. Lett. 522, 12–19.
Waldeck, A.R., Olson, H.C., Yao, W., Blättler, C.L., Paytan, A., Hodell, D.A., Johnston, D.T., 2022. Calibrating the triple oxygen isotope composition of evaporite minerals as a proxy for marine sulfate. Earth Planet. Sci. Lett. 578, 117320.
Wankel, S.D., Bradley, A.S., Eldridge, D.L., Johnston, D.T., 2014. Determination and application of the equilibrium oxygen isotope effect between water and sulfite. Geochim. Cosmochim. Acta 125, 694–711.
Whitehill, A.R., Jiang, B., Guo, H., Ono, S., 2015. SO_2 photolysis as a source for sulfur mass-independent isotope signatures in stratospheric aerosols. Atmos. Chem. Phys. 15 (5), 2569.
Wostbrock, J.A., Cano, E.J., Sharp, Z.D., 2020. An internally consistent triple oxygen isotope calibration of standards for silicates, carbonates and air relative to VSMOW2 and SLAP2. Chem. Geol. 533, 119432.
Young, E.D., Galy, A., Nagahara, H., 2002. Kinetic and equilibrium mass-dependent isotope fractionation laws in nature and their geochemical and cosmochemical significance. Geochim. Cosmochim. Acta 66 (6), 1095–1104.
Zherebker, A., Kostyukevich, Y., Volkov, D.S., Chumakov, R.G., Friederici, L., Rüger, C.P., Kononikhin, A., Kharybin, O., Korochantsev, A., Zimmermann, R., Perminova, I.V., Nikolaev, E., 2021. Speciation of organosulfur compounds in carbonaceous chondrites. Sci. Rep. 11 (1), 1–13.